*PERIODICA POLYTECHNICA SER. TRANSP. ENG. VOL. 30, NO. 1–2, PP. 37–52 (2002)*

# ROBUST CONTROL DESIGN FOR MECHANICAL SYSTEMS USING THE MIXED $\mu$ SYNTHESIS

Péter GÁSPÁR*, István SZÁSZI** and József BOKOR*

*Computer and Automation Research Institute
Hungarian Academy of Sciences
H–1111 Budapest, Kende u. 13–17, Hungary
Fax: +36 14667503
e-mail: gaspar@sztaki.hu
**Department of Control and Transport Automation
Budapest University of Technology and Economics
H–1521 Budapest, Hungary
Fax: +36 14633087
e-mail: szaszi@kaut.kka.bme.hu

Received: Sept. 20, 2002

## Abstract

The mixed $\mu$ synthesis is proposed for mechanical systems. In this method, both the real parametric and the complex uncertainties are handled together. A compensator that achieves nominal performance and meets robust stability specifications can be designed. The method will be illustrated for an inverted pendulum device as an educational example and a suspension design problem as a practical example.

*Keywords:* robust control, uncertainty, mechanical systems, automotive systems, laboratory techniques.

## 1. Introduction

In the traditional robust control design methods, usually the unmodelled dynamics, which cover the parametric uncertainties can be taken into consideration. In mechanical systems, there are several components whose parameters change around their operational points in predefined intervals. In the mixed $\mu$ method this information can be taken into consideration [2, 4, 7, 9]. The purpose of this paper is to apply the mixed $\mu$ synthesis to mechanical systems.

In the first example, a servo control is designed for an inverted pendulum. In this example the mass and the length of the rod are assumed to be uncertain with a nominal value and a range of possible variation. A model is constructed, in which both the real parametric and the complex uncertainties are taken into consideration. The control objective is to design a controller which stabilizes the rod and keeps the cart in a desired position. In the second example, an active suspension is designed based on a half-car model. Here, the sprung mass, and the suspension components are uncertain. In the control design, different performance objectives should be fulfilled, i.e. improving ride comfort, and minimizing suspension deflection.

The organization of the paper is as follows. Section 2 discusses the robust control design based on the mixed $\mu$ synthesis. Section 3 presents the servo design for an inverted pendulum and Section 4 presents the suspension design based on the half-car model. Finally, Section 5 contains some concluding remarks.

## 2. Robust Control Design Based on the Mixed $\mu$ Method

Consider the closed-loop system in *Fig. 1*, which includes the feedback structure of the model $G$ and controller $K$, and elements associated with the uncertainty models and performance objectives. In the diagram, $u$ is the control input, $y$ is the measured output, $w$ is the disturbance signal, and $n$ is the measurement noise. The $z$ represents the performance outputs.

The transfer function $\Delta_r$ contains parametric uncertainty components. The unmodelled dynamics is represented by $W_r$ and $\Delta_m$. The transfer function $W_r$ is assumed to be known, and it reflects the uncertainty in the model. The transfer function $\Delta_m$ is assumed to be stable and unknown with the norm condition, $\|\Delta_m\|_\infty < 1$. In the diagram, $e$ is the input of the perturbation, $d$ is its output. The weighting functions $W_n$ and $W_w$ represent the impact of the different frequency domains in terms of sensor noise $n$ and disturbance $w$, respectively. The weighting function $W_p$ represents the performance outputs.

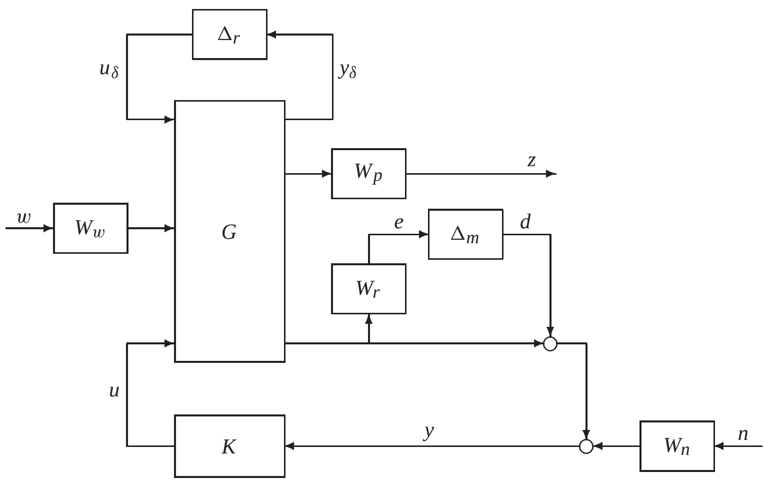


*Fig. 1.* Closed-loop interconnection structure

Necessary and sufficient conditions for robust stability and robust performance can be formulated in terms of the structured singular value denoted as $\mu$. In order to analyze the performance and robustness requirements, the closed loop system is expressed by the lower linear fractional transformation:

$$\begin{bmatrix} e \\ y_\delta \\ \hline z \end{bmatrix} = \left[\begin{array}{c|c} M_{11} & M_{12} \\ \hline M_{21} & M_{22} \end{array}\right] \begin{bmatrix} d \\ u_\delta \\ \hline w \\ n \end{bmatrix}. \tag{1}$$

The goal is to guarantee the robust performance of the closed-loop system in the face of nominal plant perturbation.

- The closed-loop system achieves the nominal performance if the following condition is satisfied:
$$\|M_{22}\|_\infty < 1. \tag{2}$$
- The closed-loop system achieves the robust stability if the following inequality is satisfied:
$$\|M_{11}\|_\infty < 1. \tag{3}$$
- The closed-loop system achieves robust performance if the performance objective is met:

$$\sup_\omega \mu(M) < 1 \Longleftrightarrow \|\mu(M)\|_\infty < 1. \tag{4}$$

The mixed real and complex $\mu$ involves three types of blocks: repeated real scalar, repeated complex scalar and full blocks. The admissible set of uncertainties $\tilde{\Delta}$ is defined as

$$\tilde{\Delta} = \begin{bmatrix} \Delta_r & 0 & 0 \\ 0 & \Delta_m & 0 \\ 0 & 0 & \Delta_p \end{bmatrix}, \tag{5}$$

The first block, $\Delta_r$ is a repeated real scalar block which represents the parametric uncertainties. The second block of this structured set corresponds to the scalar-block uncertainty $\Delta_m$, which is used to describe the unmodelled dynamics. The $\Delta_p$ is a fictitious uncertainty block, which is used to incorporate the $\mathcal{H}_\infty$ nominal performance objective into the $\mu$ framework. Given a matrix $M = \mathcal{F}_l(P, K)$, the mixed $\mu_{\tilde{\Delta}}$ function is then defined by:

$$\mu_{\tilde{\Delta}}(M) := \frac{1}{\min\{\bar{\sigma}(\Delta) : \Delta \in \tilde{\Delta},\ \det(I - M\Delta) = 0\}} \tag{6}$$

unless no $\Delta \in \tilde{\Delta}$ makes $I - M\Delta$ singular, in which case $\mu_\Delta(M) = 0$. Thus $1/\mu_{\tilde{\Delta}}(M)$ is the "size" of the smallest perturbation $\Delta$, measured by its maximum singular value, which makes $\det(I - M\Delta) = 0$.

The upper bound may be formulated as a convex optimization problem, so the global minimum can be found. An upper bound for $\mu_{\tilde{\Delta}}(M)$ that take the phase information of the real parameters into account can be formulated into an optimization problem for a constant matrix $M$ and both complex and mixed uncertainty structure $\tilde{\Delta}$:

$$\inf_{D\in\mathcal{D},\, G\in\mathcal{G}} \min_{\beta} \left\{\beta \mid M^*DM + j(GM - M^*G) - \beta^2 D \le 0\right\}. \tag{7}$$

The goal of the mixed $\mu$ synthesis is to minimize overall stabilizing controllers $K$ and the peak value $\mu_\Delta(\cdot)$ of the closed loop transfer function $\mathcal{F}_l(P, K)$. The formula is as follows:

$$\min_K \sup_\omega \mu_{\tilde{\Delta}}[\mathcal{F}_l(P, K)(j\omega)]. \tag{8}$$

Using this upper bound, the optimization is reformulated as

$$\min_K \sup_\omega \inf_{D\in\mathcal{D},\, G\in\mathcal{G}} \min_\beta \{\beta \mid \quad \bar{\sigma}(\Gamma(\omega)) \le 1\}, \tag{9}$$

$$\Gamma(\omega) = \left(\frac{D_\omega F_l(P, K)(j\omega)D_\omega^{-1}}{\beta} - jG_\omega\right)(I + G_\omega^2)^{-\frac{1}{2}}, \tag{10}$$

where $D_\omega$, $G_\omega$ are selected from the set of scaling $\mathcal{D}$, $\mathcal{G}$ independently of every $\omega$.

The scaling $G$ allows the exploitation of the phase information about the real parameters so that a better upper bound can be obtained. The optimization problem can be solved in an iterative way using for $D$, $G$ and $K$. The problem of finding $D(\omega)$, $G(\omega)$ and $\beta$ for fixed $K(s)$ is just the mixed upper bound problem. Having found these scalings $\beta^* = \max \beta$ might be fixed and transfer function matrices $D(s)$ and $G(s)$ to $D(\omega)$ and $jG(\omega)$ might be fitted. It can be shown that using spectral factorization, a stable interconnection $P_{DG}(s)$ can be formed, which approximates $\Gamma(\omega)$ across frequency $\omega$. For given $\beta^*$, $D(s)$ and $G(s)$ the problem of finding the controller $K(s)$ will be reduced to a standard $\mathcal{H}_\infty$ problem. The procedure is called $D, G - K$ iteration [1, 9].

## 3. Servo Control Design for an Inverted Pendulum

The inverted pendulum that is installed in our laboratory is shown in *Fig.2*. The cart is propelled by a DC servomotor supported by a power amplifier, the cart position and the rod angle are measured by potentiometers. The objective of the experiment is to design a controller which stabilizes the rod and keeps the cart in a desired position. Let $\bar{m}_1$ be the mass of the rod, $\bar{l}$ the length of the rod, $m_2$ the mass of the cart, $R_m$ the armature resistance, $K_m$ the motor torque constant, $K_g$ the gear-ratio of gearbox, and $r$ the radius of the gear.

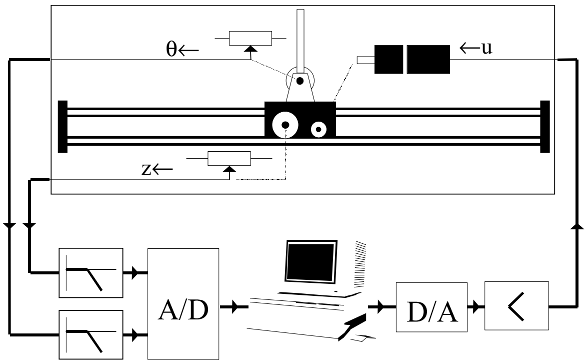


*Fig. 2.* Schematic diagram of the experiment

The state space form of the nominal model is as follows:

$$\begin{bmatrix} \dot{x}_1 \\ \dot{x}_2 \\ \dot{x}_3 \\ \dot{x}_4 \\ \hline y_x \\ y_\theta \end{bmatrix} = \left[\begin{array}{cccc|c} c_2 & \frac{1}{l} g(\frac{\bar{m}_1}{m_2}+1) & -g\frac{1}{l}c_2 & 0 & 1 \\ 1 & 0 & 0 & 0 & 0 \\ 0 & 1 & 0 & 0 & 0 \\ 0 & 0 & 1 & 0 & 0 \\ \hline 0 & c_1 & 0 & -g\frac{1}{l}c_1 & 0 \\ 0 & -\frac{1}{l}c_1 & 0 & 0 & 0 \end{array}\right] \begin{bmatrix} x_1 \\ x_2 \\ x_3 \\ x_4 \\ \hline u \end{bmatrix}, \tag{11}$$

where $x_i$'s are the state variables in the controllability state space representation form, $u$ is the input voltage, $y_x$ is the car displacement and $y_\theta$ is the rod angle [8]. In *Eq.* (11), the $c_1 = \frac{K_g K_m A_m}{R_m m_2 r}$ and $c_2 = -\frac{K_g^2 K_m^2}{R_m m_2 r^2}$ are constants.

The parametric uncertainties are generated in a laboratory environment by varying the length of the rod $l$ and its mass $m_1$. The parameters are assumed to be uncertain, with a nominal value and a range of possible variation:

$$m_1 = \bar{m}_1(1 + d_m \delta_m), \quad l = \bar{l}(1 + d_l \delta_l) \tag{12}$$

with $d_m$, $d_l$ scalars, in which $-1 \leq \delta_m,\ \delta_l \leq 1$. The $d$ scalar indicates the percentage of variation that is allowed for a given parameter around its nominal value. The changing of $\delta$ parameters in the interval $\left[\, {\scriptstyle -1\ 1} \,\right]$ determines the actual parameter deviation. All uncertainty parameters can be written in lower Linear Fractional Transformation (LFT) form. The $l$ parameter occurs in the denominator of the differential equation so its LFT representation is as follows:

$$\frac{1}{l} = \frac{1}{\bar{l}(1 + d_l \delta_l)} = \mathcal{F}_l\left(\begin{bmatrix} \frac{1}{\bar{l}} & -\frac{d_l}{\bar{l}} \\ 1 & -d_l \end{bmatrix}, \delta_l\right) = \mathcal{F}_l(M_l, \delta_l). \tag{13}$$

The $m_1$ occurs in the numerator and their LFT representation can be drawn up in the following way:

$$m_1 = \bar{m}_1(1 + d_m\delta_m) = \mathcal{F}_l\left(\begin{bmatrix} \bar{m}_1 & 1 \\ d_m\bar{m}_1 & 0 \end{bmatrix}, \delta_m\right) = \mathcal{F}_l(M_m, \delta_m). \tag{14}$$

The $\delta$ uncertainty blocks from the motion equations must be pulled out. Let the input and output of $\delta_m$ be $y_{m_1}$ and $u_{m_1}$, and $\delta_l$ be $y_l$ and $u_l$, respectively. In the differential equations of the nominal plant the length of the rod $l$ occurs in several times. In general such parameters can only be treated as a repeated scalar block. It means that different uncertain parameters must be handled by the same uncertain coefficients $(d, \delta)$. Thus, $l$ can be modelled as a three times repeated parameter. The $u_l^i$ and $y_l^i$ $(i = 1, 2, 3)$ represent the input and output signals of the length uncertainty, and $u_m^i$, $y_m^i$ represent the signals of the mass uncertainty.

Applying *Eqs.* (13) and (14), the state space form containing uncertain parameters can be formulated in the following way. The uncertain state space model in which $M_m$ and $M_l$ are the uncertain blocks is shown in *Fig.* 3.

$$\begin{bmatrix} \dot{x}_1 \\ \dot{x}_2 \\ \dot{x}_3 \\ \dot{x}_4 \\ \hline y_l^1 \\ y_l^2 \\ y_l^3 \\ y_m^1 \\ \hline y_x \\ y_\theta \end{bmatrix} = \left[\begin{array}{cccc|cccc|c} c_2 & \frac{1}{l}g(\frac{\bar{m}_1}{m_2}+1) & -g\frac{1}{l}c_2 & 0 & -\frac{d_l}{l}g(\frac{\bar{m}_1}{m_2}+1) & -\frac{d_l}{l}c_2 & 0 & \frac{1}{m_2}g & 1 \\ 1 & 0 & 0 & 0 & 0 & 0 & 0 & 0 & 0 \\ 0 & 1 & 0 & 0 & 0 & 0 & 0 & 0 & 0 \\ 0 & 0 & 1 & 0 & 0 & 0 & 0 & 0 & 0 \\ \hline 0 & 1 & 0 & 0 & -d_l & 0 & 0 & 0 & 0 \\ 0 & 0 & -g & 0 & 0 & -d_l & 0 & 0 & 0 \\ 0 & 0 & 0 & 1 & 0 & 0 & -d_l & 0 & 0 \\ 0 & \frac{1}{l}d_m\bar{m}_1 & 0 & 0 & -\frac{d_l}{l}d_m\bar{m}_1 & 0 & 0 & 0 & 0 \\ \hline 0 & c_1 & 0 & -g\frac{1}{l}c_1 & 0 & 0 & g\frac{d_l}{l}c_1 & 0 & 0 \\ 0 & -\frac{1}{l}c_1 & 0 & 0 & \frac{d_l}{l}c_1 & 0 & 0 & 0 & 0 \end{array}\right] \begin{bmatrix} x_1 \\ x_2 \\ x_3 \\ x_4 \\ \hline u_l^1 \\ u_l^2 \\ u_l^3 \\ u_m^1 \\ \hline u \end{bmatrix} \tag{15}$$

The control design based on the $\mu$ synthesis is performed in two ways. The first approach is based on the complex $\mu$ synthesis, in which the model uncertainties are represented by complex frequency dependent $\Delta$ blocks and a priori information about the real parametric uncertainties is not used in the design process. The second approach is based on the mixed $\mu$ synthesis, in which the real parametric uncertainties are taken into consideration, i.e. both the complex and the real frequency independent uncertainties are handled in $\Delta$ blocks. The nominal parameters of the inverted pendulum are shown in *Table* 1.

Let the required transfer function from the reference to the displacement of the cart be the following simple first-order system: $T_{yr} = \frac{1}{s+1}$. The reference tracking should ideally be decoupled at the output channels and must fulfil the requirements determined in the time domain. In order to meet our requirements for the tracking error, let's apply a $W_e$ weighting function, which reduces the steady state error below 1%: $W_e = 100\frac{s/7+1}{s/0.02+1}$. According to the condition the transfer function

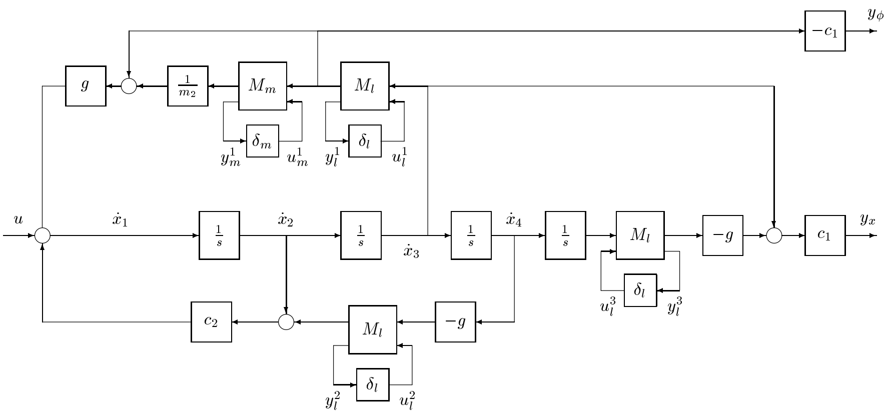


*Fig. 3.* Block structure of the uncertain model

*Table 1.* Parameters of the inverted pendulum

| Parameters (symbols) | Value |
|---|---|
| Mass of the rod ($m_1$) | 0.210 kg |
| Length of the rod ($l$) | 0.305 m |
| Mass of the cart ($m_2$) | 0,455 kg |
| Armature resistance ($R_m$) | 2.6 $\omega$ |
| Motor torque constant ($K_m$) | 0.00767 Nm |
| Gear-ratio of gearbox ($K_g$) | 3.7 |
| Radius of the gear ($r$) | 0.00635 m |

from the reference signal to the cart position must be less than $1/W_e$ in the $\mathcal{H}_\infty$ norm sense, i.e. less than $\frac{1}{100}$ in steady state. Let the frequency weighting function of the control input be $W_u = \frac{1}{20}$. The fact that the magnitude of the reference signal is 0.2 m entails that the effect of the reference signal on the control input will not exceed 26 dB. It is assumed that the sensor noise is 5 mm in the cart position and 0.01 rad in the rod angle in the entire frequency domain, thus the weighting function of the sensor noise is represented by $W_n = \begin{bmatrix} 0.005 & 0 \\ 0 & 0.01 \end{bmatrix}$. It is assumed that disturbances at the angle should be rejected by a factor of 5 by using $W_p = 5\frac{s/2+1}{s/0.1+1}$ in the low frequency domain..

In the mixed $\mu$ approach, information about the model uncertainties between the model and the plant must be used in the control design, and the magnitude of the unmodelled dynamics is reduced. Thus the uncertainties are selected in the following way: $W_r = 0.1\frac{s/8+1}{s/110+1}$. It means that the modelling error is about 10%

in the low frequency domain and, it is up to 100% in the upper frequency domain.

The mixed $\mu$ synthesis is performed by using the $D, G - K$ iteration. The values of the iteration steps are shown in *Table* 2. As a result of Step 3, the compensator order is selected 44, and all the nominal performance, the robust stability, and the robust performance are achieved. The price of the mixed $\mu$ synthesis is usually a controller with rather large order, which can usually be reduced. The controller reduction method is based on the balanced realization and optimal Hankel norm approximation [6]. The order of the controller reduced is selected 12.

Using a simulation procedure, the step responses and the impulse responses are shown in *Fig. 4*. As it is shown, the designed compensator guarantees the tracking of the reference signal, small interaction between the signals, and minimal input voltage. The properties of the disturbance attenuation are also analyzed for both cases by using 0.1 rad impulse to the angle channel. As the impulse responses show, in both cases the effect of the disturbance is attenuated during the specified interval.

*Table 2.* Summary of the $D$,$G$–$K$ iteration

| Iteration | #1 | #2 | #3 |
|---|---|---|---|
| Controller order | 8 | 22 | 44 |
| $D$-scale order | 0 | 14 | 24 |
| $G$-scale order | 0 | 0 | 12 |
| Gamma achieved | 33.755 | 1.183 | 1.011 |
| Peak $\mu$ value | 2.193 | 1.166 | 0.977 |

## 4. Active Suspension Design

The well-known rigid half-car vehicle model, which is shown in *Fig.* 5, is widely used for active suspension design. The model comprises three parts: the sprung mass and two unsprung masses. Let the sprung and unsprung masses be denoted by $m_s$, $m_{uf}$, $m_{ur}$, respectively. Both suspensions consist of a linear spring, a damper and an actuator to generate a pushing force between the body and axle. The front and rear suspension stiffness, the front and rear tire stiffness are denoted by $k_{sf}$, $k_{sr}$ and $k_{tf}$, $k_{tr}$, respectively. The front and rear suspension dampings are denoted by $b_{sf}$, $b_{sr}$.

The half-car model is a four degrees-of-freedom system. The sprung mass is assumed to be a rigid body and has freedom of motion in the vertical and pitch direction. The $x_1$ denotes the vertical displacement at the center of gravity and $\theta$ is the pitch angle of the sprung mass. The front and rear displacements of the sprung and the unsprung masses are denoted by $x_{1f}$, $x_{1r}$ and $x_{2f}$, $x_{2r}$. In the model, the disturbances, $w_f$, $w_r$ are caused by road irregularities. The input signals, $f_f$, $f_r$

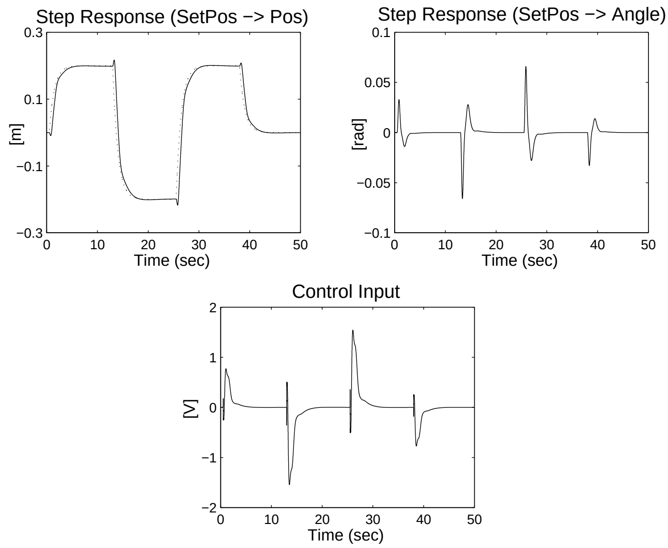


(a) Step responses of the controlled system

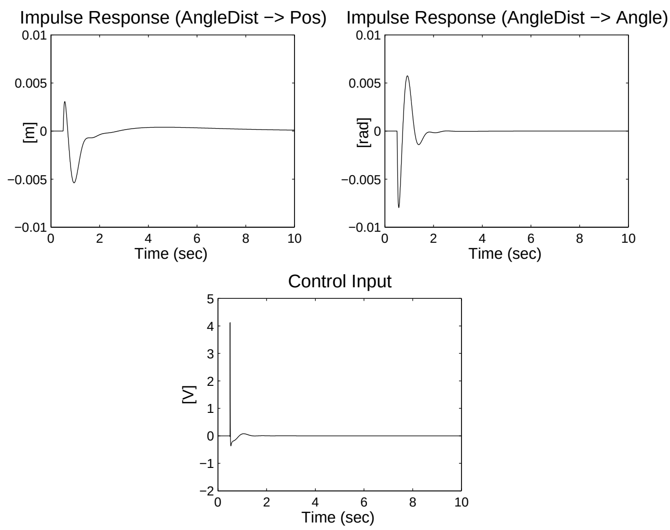


(b) Impulse responses of the controlled system

*Fig. 4.* Simulation results of the controlled system

are generated by the actuators.

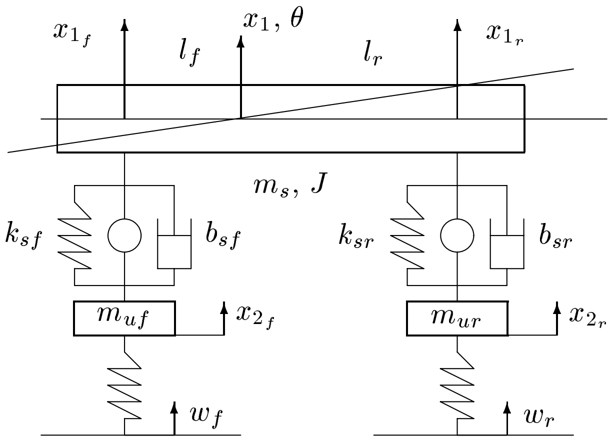


*Fig. 5.* Rigid half-car model

In this example the sprung mass and the tire stiffness are assumed to be uncertain in the following way:

$$m_s = \bar{m}_s(1 + d_{m_s}\delta_{m_s}), \tag{16}$$

$$k_i = \bar{k}_i(1 + d_{k_i}\delta_{k_i}), \tag{17}$$

where $i \in \{sf,\ sr,\ tf,\ tr\}$ and $d_{m_s}, d_{k_i}$ scalars, in which $-1 \leq \delta_{m_s},\ \delta_{k_i} \leq 1$. The $d$ scalar indicates the percentage of variation that is allowed for a given parameter around its nominal value. The changing of $\delta$ parameters in the interval $\begin{bmatrix}-1 & 1\end{bmatrix}$ determines the actual parameter deviation. All uncertainty parameters can be written in lower Linear Fractional Transformation (LFT) form. The $m_s$ parameter occurs in the denominator of the motion differential equation, and the other uncertainty parameters such as $k_i$ occur in the numerator. Their LFT representation can be represented in the following way:

$$\frac{1}{m_s} = \mathcal{F}_l\left(\begin{bmatrix}\frac{1}{\bar{m}_s} & -\frac{d_{m_s}}{\bar{m}_s}\\ 1 & -d_{m_s}\end{bmatrix}, \delta_{m_s}\right), \tag{18}$$

$$k_i = \mathcal{F}_l\left(\begin{bmatrix}\bar{k}_i & 1\\ d_{k_i}\bar{k}_i & 0\end{bmatrix}, \delta_{k_i}\right). \tag{19}$$

The $\delta$ uncertainty blocks must be pulled out from the motion differential equations. Let the input and output of $\delta_{m_s}$ be $y_{m_s}$ and $u_{m_s}$, and $\delta_{k_i}$ be $y_{k_i}$ and $u_{k_i}$, respectively.

Applying these formulae, the motion equation can be drawn up in the following way:

$$M\ddot{z} + B\dot{z} + Kz = Fu_\delta + K_r w + G_a f, \tag{20}$$

where

$$z = \begin{bmatrix} x_1 & \theta & x_{2f} & x_{2r} \end{bmatrix}^T, w = \begin{bmatrix} w_f & w_r \end{bmatrix}^T,$$
$$f = \begin{bmatrix} f_f & f_r \end{bmatrix}^T, u_\delta = \begin{bmatrix} u_{m_s} & u_{k_{sf}} & u_{k_{sr}} & u_{k_{tf}} & u_{k_{tr}} \end{bmatrix}^T,$$

and the matrices are as follows:

$$M = \begin{bmatrix} M_s & 0 \\ 0 & M_u \end{bmatrix}, B = \begin{bmatrix} GB_sG^T & -GB_s \\ -B_sG^T & B_s \end{bmatrix}, G_a = \begin{bmatrix} -G \\ I \end{bmatrix},$$
$$K = \begin{bmatrix} GK_sG^T & -GK_s \\ -K_sG^T & K_s + K_t \end{bmatrix}, K_r = \begin{bmatrix} 0 \\ K_t \end{bmatrix}, F = \begin{bmatrix} F_1 \\ F_2 \end{bmatrix}.$$

Here the sprung mass ($M_s$), the unsprung mass ($M_u$), the suspension stiffness ($K_s$), the tire stiffness ($K_t$), suspension damping ($B_s$), geometry ($G$) and ($F_1$, $F_2$) matrices are as follows:

$$M_s = \begin{bmatrix} \bar{m}_s & 0 \\ 0 & I_\theta \end{bmatrix}, M_u = \begin{bmatrix} m_{uf} & 0 \\ 0 & m_{ur} \end{bmatrix}, B_s = \begin{bmatrix} b_{sf} & 0 \\ 0 & b_{sr} \end{bmatrix},$$
$$K_s = \begin{bmatrix} \bar{k}_{sf} & 0 \\ 0 & \bar{k}_{sr} \end{bmatrix}, K_t = \begin{bmatrix} \bar{k}_{tf} & 0 \\ 0 & \bar{k}_{tr} \end{bmatrix},$$
$$G = \begin{bmatrix} 1 & 1 \\ l_f & -l_r \end{bmatrix}, F_1 = \begin{bmatrix} \begin{bmatrix} -d_{m_s} \\ 0 \end{bmatrix} & G & 0 \end{bmatrix}, F_2 = \begin{bmatrix} 0 & I & I \end{bmatrix}.$$

Using the differential equation (20) the state equation can be formulated in the following way:

$$\dot{x} = \hat{A}x + \hat{B}_1 w_\delta + \hat{B}_2 f, \tag{21}$$

where

$$x = \begin{bmatrix} z^T & \dot{z}^T \end{bmatrix}^T, \quad w_\delta = \begin{bmatrix} u_\delta^T & w^T \end{bmatrix}^T,$$
$$\hat{A} = \begin{bmatrix} 0 & I \\ -M^{-1}K & -M^{-1}B \end{bmatrix}, \quad \hat{B}_1 = \begin{bmatrix} 0 & 0 \\ M^{-1}F & M^{-1}K_r \end{bmatrix}, \quad \hat{B}_2 = \begin{bmatrix} 0 \\ M^{-1}G_a \end{bmatrix}.$$

In the demonstration example, the suspension design is based on a half-car model, the nominal parameters of which are shown in *Table*3. In the example, the dynamics of the hydraulic actuator are modelled as $G_a(s) = \frac{1}{1/75s+1}$. The parameters are

*Table 3.* Parameters of the half-car model

| Parameters (symbols) | Value |
|---|---|
| Sprung mass ($m_s$) | 580 kg |
| Pitch moment inertia ($I_\theta$) | 1100 kg·m$^2$ |
| Front (rear) unsprung mass ($m_{uf}$) | 40 kg (40 kg) |
| Front suspension stiffness ($k_{sf}$) | 23500 N/m |
| Rear suspension stiffness ($k_{sr}$) | 25500 N/m |
| Front tire stiffness ($k_{tf}$) | 190000 N/m |
| Rear tire stiffness ($k_{tr}$) | 190000 N/m |
| Front suspension damping ($b_{sf}$) | 1000 N/m/s |
| Rear suspension damping ($b_{sr}$) | 1100 N/m/s |

assumed to be uncertain, with a nominal value and a range of possible variation: $d_{ms} = 0.2, d_{ksf} = 0.15, d_{ksr} = 0.15, d_{ktf} = 0.25, d_{ktr} = 0.25$. Note that this represents 20% uncertainty in $m_s$, 15% uncertainty in $k_{sf}$ and $k_{sr}$, moreover 25% uncertainty in $k_{tf}$ and $k_{tr}$.

In preparation for the control design, the uncertainty weighting function $W_r$ and the performance weighting function $W_p$ must be selected. In the mixed $\mu$ synthesis, in which mixed uncertainty is applied, information about the model uncertainties between the model and the plant must be used in the control design. Thus, the weighting function $W_r$ can be selected in the following way: $W_r = 0.2\frac{S+50}{S+200}$.

The purpose of the weighting functions $W_{p_1}$, $W_{p_2}$ and $W_{p_3}$ is to keep the vertical and pitch acceleration, moreover, to keep the suspension deflection small over the desired frequency range. We choose $W_{p_1} = W_{p_2} = 0.2\frac{S+200}{S+50}$, and $W_{p_3} = \mathrm{diag}\left[0.029\frac{S+350}{S+10}, 0.029\frac{S+350}{S+10}\right]$ for front and rear suspension, respectively. Let the frequency weighting function for the wheel travel be $W_{p_4} = \mathrm{diag}\,[1, 1]$. The magnitude of the control force is limited by the weighting function $W_{p_5} = \mathrm{diag}\left[4 \cdot 10^{-3}, 4 \cdot 10^{-3}\right]$. The weight $W_w$ is used to scale the magnitude of the road disturbance, which is chosen $W_w = 0.03$. The fact that the magnitude of the road excitation is 0.03 m entails that the effect of the disturbance signal on the control input will not exceed 48 dB. We set $W_n = 0.001$, thus essentially it is assumed that the sensor noise is 0.001 m/s$^2$ at the front and rear body acceleration in the whole frequency domain.

In the synthesis, the control design is performed by using the $D, G - K$ iteration method. The values of the steps of the iteration are shown in *Table 4*. Because of Step 3, the compensator order is selected 68. The price of the mixed $\mu$ synthesis is usually a controller with larger order, which can usually be reduced. The controller reduction is based on the balanced realization and optimal Hankel norm approximation. The order of the controller is selected 20, in which all the nominal performance, the robust stability, and the robust performance are achieved.

*Table 4*. Summary of the $D,G$–$K$ iteration

| Iteration | #1 | #2 | #3 |
|---|---|---|---|
| Controller order | 16 | 32 | 68 |
| $D$-scale order | 0 | 16 | 30 |
| $G$-scale order | 0 | 0 | 22 |
| Gamma achieved | 5460.07 | 19.166 | 1.327 |
| Peak $\mu$ value | 44.253 | 1.413 | 0.991 |

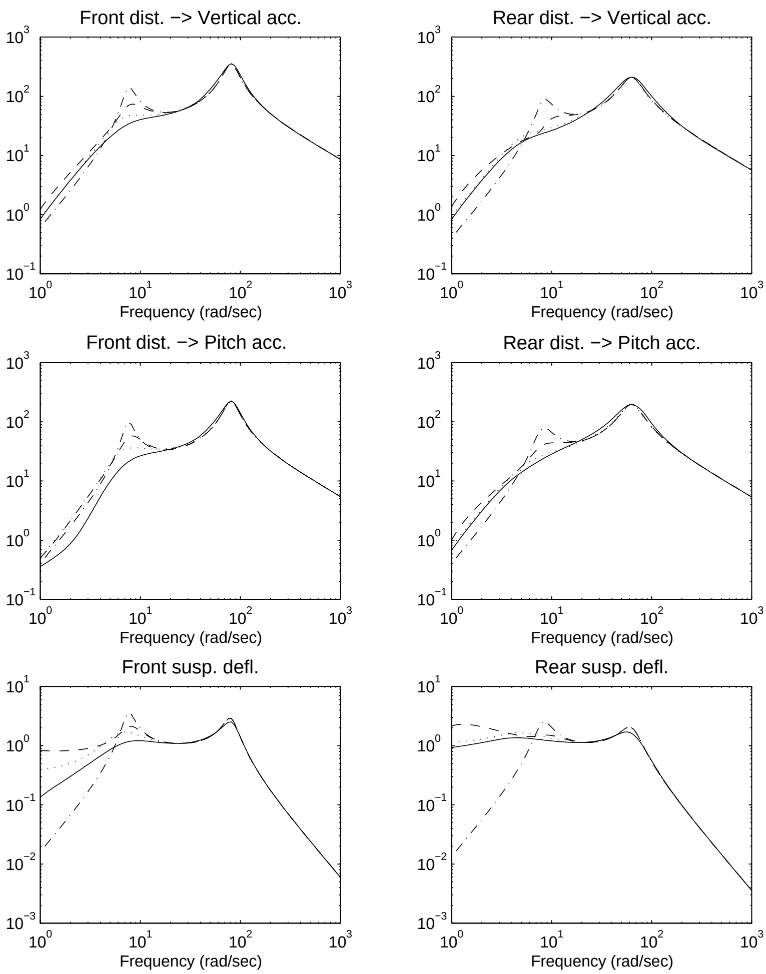


*Fig. 6.* Frequency responses of the designed system

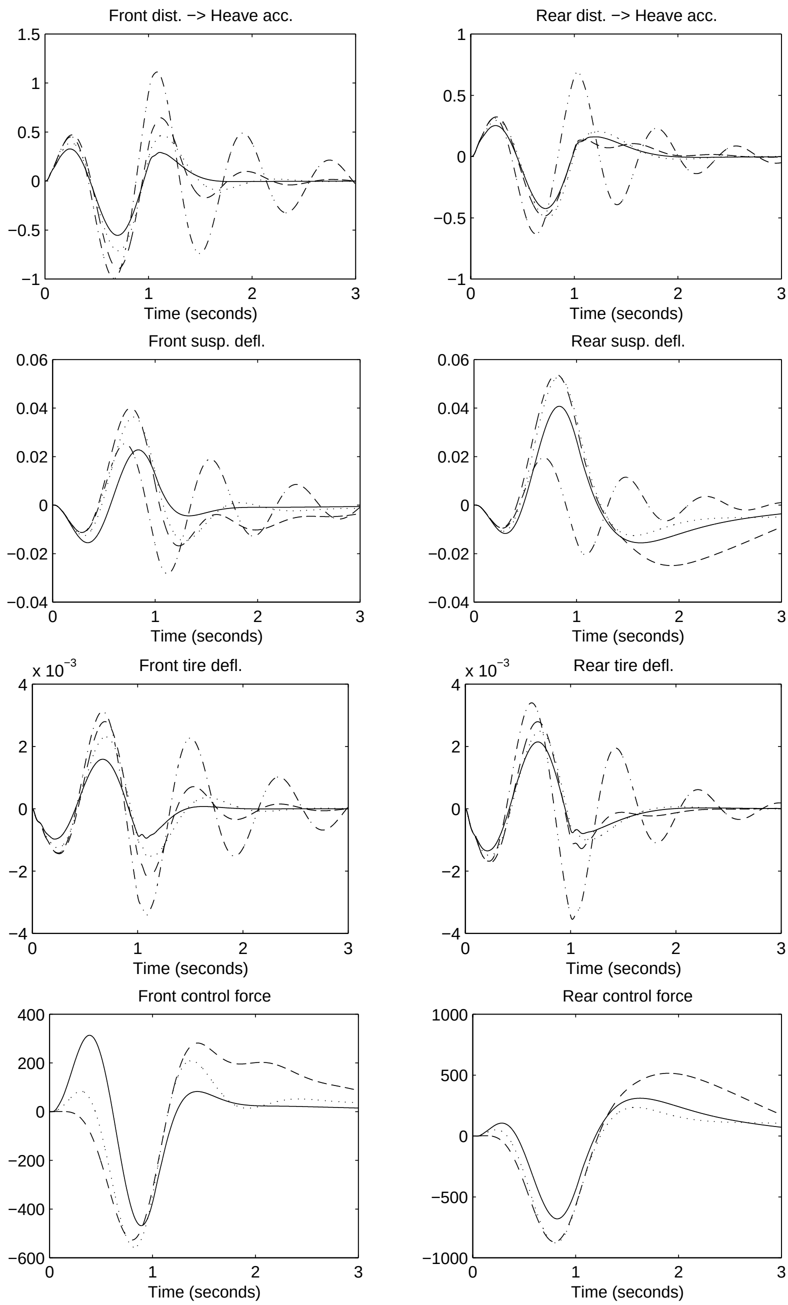


*Fig. 7.* Time responses of the designed system

The frequency responses of the controlled system, i.e. the vertical accelerations, the pitch accelerations, and the suspension deflection are illustrated in *Fig.*6. The solid line corresponds to the mixed $\mu$ synthesis, the dashed line to the complex $\mu$ synthesis, the dotted line to the LQG design, and the dashed-dotted line to the passive system. The first amplitude peak, which corresponds to the eigenfrequency of the body mass, is the largest in the passive system, and it practically disappears in the mixed $\mu$ design. The reduction in vertical and pitch acceleration in the low frequency range corresponds to the increase in the suspension deflection in this range. Since the tire-hop frequency is an invariant point (about $\omega_1 = 68.9$ rad/sec in this example), the acceleration responses are close to the passive response at this frequency and they cannot be decreased by feedback.

The designed compensators are verified in the time domain (see *Fig.* 7). In the example, the input signal is simulated as a bump with 0.03 m maximal value. The effects of the disturbance on the sprung mass acceleration are seen as large oscillations with long duration in the case of complex $\mu$ control. The mixed $\mu$ control shows better properties in terms of both the value and the duration of the oscillations. The effects of the disturbance on the suspension deflection are great in the complex $\mu$ control. In the mixed $\mu$ case, the suspension deflection achieves its steady state value within a short time. The overshoot of the LQG control is the largest, however, the duration is shorter than in the complex $\mu$ case. The input forces are similar in all cases. The mixed $\mu$ control requires the largest input force, however, it achieves its steady state value shortly without any oscillation. The duration of the force oscillation is long in the case of both the LQG and the complex $\mu$ control systems.

## 5. Conclusions

In this paper, the mixed $\mu$ synthesis has been presented through two case studies. The magnitude of the unmodelled dynamics between the model and the plant can be reduced if real parametric uncertainties are taken into consideration. It means that information about the parametric uncertainties must be used in the control design. As a consequence the bandwidth of the controlled system can be increased in case of the mixed $\mu$. The price of the mixed $\mu$ synthesis is usually a controller with a large order, however, it can be effectively reduced by using a controller reduction method.

## Acknowledgement

This work was supported by the Hungarian National Science Foundation (OTKA) under the grant #T030182 which is gratefully acknowledged.

## References


[1] BALAS, G. – DOYLE, J. C. – GLOVER, K. – PACKARD, A. – SMITH, R., $\mu$ Analysis and Synthesis Toolbox, *MUSYN Inc. and The Mathworks Inc.* (1991).

[2] DOYLE, J., Structured Uncertainties in Control System Design, *Proc. of the 24th Conference on Decision and Control*, Lauderdale, (1 985), pp. 260–265.

[3] DOYLE, J. C. – PACKARD, A., Uncertainty Multivariable Systems from a State Space Perspective, In *Proc. American Control Conf.*, Minneapolis, (1987), pp. 2147–2152.

[4] FAN, M. K. H. – TITS, A. L. – DOYLE, J. C., Robustness in the Presence of Mixed Parametric Uncertainty and Unmodelled Dynamics, *Trans. Automatic Control*, **AC–36**, No. 1, (1991), pp. 25–38.

[5] GÁSPÁR, P. – SZÁSZI, I., Robust Servo Control Design Using Identified Models, *Proc. of the 3rd IFAC Symposium on Robust Control Design*, Prague, Czech Republic, W3B-27, (2000).

[6] GLOVER, K., All Optimal Hankel Norm Approximations of Linear Multivariable Sytems and their $L_\infty$ Error Bounds, *International Journal of Control*, **39** (1984), pp. 1115–1193.

[7] PACKARD, A. – DOYLE, J., The Complex Structured Singular Value, *Automatica*, **29** No. 1 (1993), pp. 71–109.

[8] SOUMELIDIS, A. – GÁSPÁR, P. – BOKOR, J., Inverted Pendulum. An Environment for Intelligent Control Design and Test, *Proc. of the 3rd IFAC Symp. on Intelligent Components*, Annecy, (1997), pp. 421–425.

[9] ZHOU, K. – DOYLE, J. C., *Robust and Optimal Control*, Prentice Hall, New Jersey, 1996.

[10] YOUNG, P. M. – NEWLIN, M. P. – DOYLE, J. C., $\mu$ Analysis with Real Parametric Uncertainty, In *Proc. 30th IEEE Conf. on Decision and Control.*, Brighton, England, (1991), pp. 1251–1256.